5 Results on nanowire synthesis and characterization

Platinum nanowires have been synthesized by various techniques including template electrodeposition, chemical reduction, and electrospinning.[145,148,149] Other shape controlled Pt nanostructures have been generated by a number of methods.[7,9,150,151] Here, results on the fabrication of Pt nanowires by the ion-track template electrodeposition method and on the morphology of the obtained structures are presented. Properties arising from the dimensions and the structure are discussed including electrical transport properties and thermal stability. In addition, methods to precisely tune their structure by adopting known substructuring techniques and by introducing novel methods are demonstrated.

In the following section, the synthesis of Pt nanowires by template electrodeposition into ion-track etched polycarbonate membranes is reported. Studies are performed to elucidate the possibilities provided by this conventional method and perform characterizations to identify and overcome current limitations.

5.1 Pt nanowires by template based method

Since electrodeposition in ion-track etched polycarbonate membranes is a frequently used method, the challenge of synthesizing Pt nanowires by this method lies within the determination of the deposition conditions and the optimization of the nanowire structures. The production has been described in a previous work by Rauber.[19] Therefore, this section is focused on novel results, while important aspects that have been previously reported are briefly summarized.
Although the ion-track template method constitutes a well-known synthesis approach for other materials, it is essential to investigate the possibilities of this conventional method for Pt nanostructures in order to advance the fabrication process. Thus, the obtained results become the basis not only for improved Pt nanowires in terms of structure and morphology, but also may contribute to the development of complex Pt nanowire assemblies.

5.1.1 Fabrication and Characterization

Pt nanowires were synthesized by template electrodeposition from a electrolyte solution using a two-electrode electrochemical cell as described in section 4.1.2. Polycarbonate has been employed as template material for Pt nanowire fabrication in previous reports, e.g., by Choi et al. who applied an acidic solution containing H_2PtCl_6 as Pt species.[145] In this thesis, primarily an alkaline electrolyte based on $Na_2[Pt(OH)_6]$ (Platin-OH) is used. This electrolyte bath proved to be suitable to achieve high filling rates of the nanochannels and shows an excellent efficiency regarding the deposition reaction of approximately 100%. Nanowire arrays were grown in polycarbonate templates of different thicknesses and various nanochannel densities exhibiting randomly distributed channel openings across the polymer surface. The voltage was potentiostatically applied or adjusted as a periodic function of time (PED, PR) at temperatures up to 65 °C.

In Figure 5.1a-b, representative micrographs of Pt nanowires that were produced by applying different electrodeposition parameters at 65 °C are shown. After template removal, the 30 µm long nanowires with an average diameter of 40 nm, which were grown using dc plating, are randomly distributed on the substrate (Figure 5.1a). In the inset, the wires are depicted at higher magnification and reveal their continuously cylindrical shape with constant diameter along the wire axis.

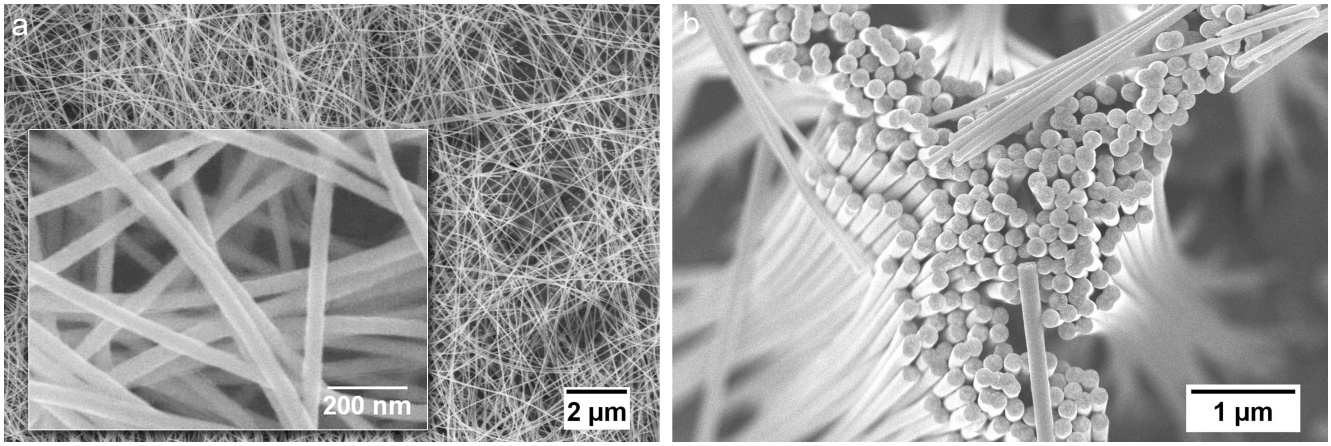

Figure 5.1: FESEM images of Pt nanowires produced by template electrodeposition in 30 μm thick PC membranes: (a) Randomly distributed nanowires fabricated by dc deposition at -1.3 V at 65 °C. The inset shows the same wires at higher magnification revealing a cylindrical shape along the wire axis. (b) Conical wires were grown using pulsed electrodeposition at 65 °C.

Table 5.1: Overview on deposited nanowire arrays with nanowire dimensions and integration densities.

Template thickness [μm]	Integration density [wires/cm^2]	Wire radius [nm]
10	1x10^9 - 1x10^{10}	10 - 30
30	1x10^7 - 5x10^9	15 - 350
60	1x10^5 - 1x10^8	70 - 300
100	1x10^3 - 1x10^8	80 - 400

The surface of the nanowires seems to be very smooth. The precise replication of the nanochannel shape is possible because of the polycrystalline structure of the nanowires consisting of very small grains. A detailed investigation of grain sizes and textures of electrodeposited Pt nanowires, based on XRD and TEM analysis, is presented in section 5.2.2.

Cylindrical nanowires were produced in PC membranes of different thickness ranging from $10-100$ µm. The nanowires with the smallest radius of r=10 nm were produced in a 10 µm template. Integration densities of up to 1x10^{10} wires/cm^2 were realized. The obtained wire dimensions are summarized in Table 5.1.

Due to the characteristics of the template materials, the diameter distribution of the nanowires was considerably narrow with a typical value of 7-11% for the standard deviation. Histogramms illustrating the distribution of the diameter are shown in Figures 5.2a-b for nanowire samples with an average diameter of 30.0 and 73.8 nm, respectively. The distribution for 49.5 nm diameter nanowires is given in the appendix (Supporting information, Figure S5). The scatter in nanowire diameter slightly increases as the average diameter decreases. The same trend is observed for increasing template thicknesses. The effect of nanochannel density on the distribution was not considered.

In Figure 5.1b, conical nanowires that were synthesized using pulsed electrodeposition (PED) at 65 °C are imaged (see also Supporting information, Figure S1a). For nanowire growth, a deposition pulse was applied at U_1=−1 V followed by a second pulse at U_2=−0.15 V during which no deposition took place. The pulse durations were adjusted to reduce the growth rate resulting in a total depostion time of >4 h. While nanowires produced by dc depostion with a relative short depostion time ($\leq$2 h) appear cylindrical in shape, PED techniques result in conical nanowires if the deposition time is considerably longer. The fact that conical wire geometries are observed at long deposition times can be explained by the used electrolyte solution with a high pH value. The alkaline Pt bath continues the chemical etching

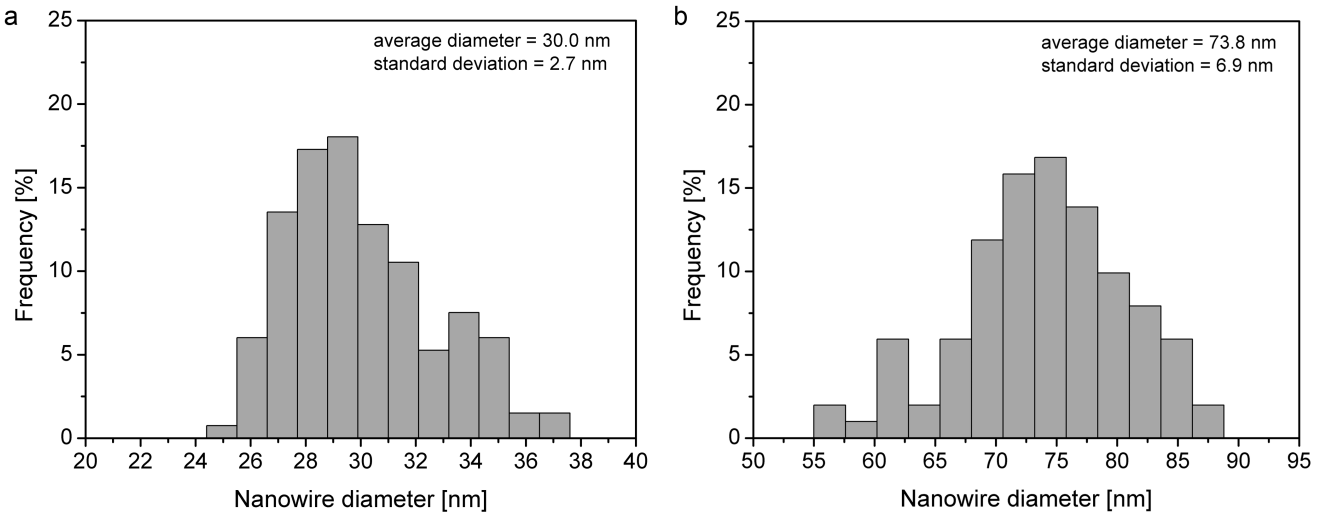

Figure 5.2: Histogramm illustrating the diameter distribution of Pt nanowires prepared in 30 μm thick polycarbonate membranes. More than 100 randomly selected nanowires grown at different areas of the template were investigated by FESEM. (a) For nanowires with an average diameter of 30 nm the standard deviation is 9% with respect to the average diameter. (b) Wires with d=73.8 nm show the same relative deviation in diameter. Absolute values are given in the graphs.

of the polymer foil at a slower rate than during the template fabrication process. Because the etching rate is much slower, effects on the wire shape (originating from the channel geometry) are observed only in the case of long deposition times at elevated temperatures; strictly cylindrical nanowires can be easily produced by keeping the deposition process short.

Conical nanowires are also obtained for dc plating at reduced potentials, resulting in a slower deposition process, and hence a reduced growth rate.

The slowly proceeding etching process, driven by the electrolyte solution, could be purposefully employed to produce conical nanowires with controlled cone angles. The longer the deposition time, the larger becomes the cone angle. Using appropriate experimental conditions, the template fabrication can be carried out *in situ*. Furthermore, it is possible to introduce cylindrical segments that vary in diameter by sequentially stopping the deposition process during wire growth to allow the electrolyte to stepwise increase the channel dimensions (Supporting information, Figure S1b).

5.1.2 Transport properties

Transport properties of Pt nanowires produced within this thesis were analyzed in collaboration with the Völklein group at University of Applied Sciences Wiesbaden (Rüsselsheim).[45] They developed a microchip to contact single nanowires for the measurement of their thermal and electrical conductivity.

The investigations on polycrystalline Pt nanowires resulted in the following main conclusions: (i) Both electrical and thermal conductivities of the nanowires (σ_{nw} and λ_{nw}, respectively) are reduced in comparison to the bulk values. While σ_{nw} is reduced by a factor of 2.5 compared to the Pt bulk value $\sigma_0 = 9.6\text{x}10^6\ (\Omega\ \text{m})^{-1}$ at 295 K, λ_{nw} is decreased by 3.4 (λ_0=71 W/m K). As a consequence, the Lorenz number of the Pt nanowires is also smaller than the bulk Lorenz number. (ii) In addition, a decrease was observed for the temperature coefficient of resistivity β (TCR).

The decrease in electrical conductivity can be explained by classical size effects. Due to the small grain size measured for the Pt nanowires an increased contribution of electron scattering at grain boundary is expected. According to the Mayadas-Shatzkes model, the carrier mobility depends on the electron

mean free path l_e, the mean grain size D_g, and the grain boundary reflection coefficient R_g (Equation 2.18).[87] Because D_g is smaller in Pt nanowires than in bulk Pt, reduced values are obtained for transport processes governed by electrons.

5.1.3 Thermal stability

The investigation of the stability of Pt nanostructures at elevated temperatures is of particular importance because Pt nanowire building blocks are of great interest for advanced technological applications. Regardless whether they will be employed as functional elements in devices used in the field of catalysis, sensing, or electrical circuits, elevated temperatures have to be expected.

Here, we study the stability of cylindrical Pt NWs against heat and transformation processes. The Rayleigh instability of electrodeposited Pt nanowires has not been investigated so far. Understanding the fragmentation and the underlying mass transport processes is of fundamental importance to avoid decay and assure satisfactory durability of Pt nanowire-based devices.
These investigations can help to complement the scarcely available results on Rayleigh decay of nanowires and provide the opportunity to further develop theoretical considerations.

Annealing experiments

To systematically investigate thermal stability and the related morphological transformations, controlled annealing experiments were performed with Pt nanowires. The nanowires were produced following the dc method described in section 4.1 resulting in parallel aligned arrays of polycrystalline nanowires with a continuously cylindrical geometry. The template was dissolved in CH_2Cl_2, and nearly all polymer residues were removed by repeatedly changing the solvent. The cleaned wires, still connected with the Au/Cu cathode layer as shown in Figure 5.3a, were disconnected and dispersed in dichloromethane using ultrasound. Subsequently, the nanowires were transfered on a SiO_2 substrates by pipetting a few drops of the CH_2Cl_2 solution onto the substrate surface. Figure 5.3b depicts an isolated Pt nanowire on the plain substrate imaged by FESEM after the solvent had been evaporated. The inset shows the same wire at higher magnification highlighting the cylindrical shape.

The prepared samples were heated in an evacuated tube furnace to different temperatures T_h within 30 minutes. The temperature was held for a fixed time t_a and cooled down to room temperature. Nanowires of different diameters (d=30, 50, and 74 nm) were heated and analyzed by FESEM before and after the annealing process.

Morphological evolution

The morphology of the wires underwent significant changes during the annealing process. All observed nanowires became unstable and finally decayed into chains of spheres when increasing the temperature to sufficient high values. At 1000 °C – a temperature much below the melting point of bulk platinum (1768 °C) – all observed nanowires formed spheres. The fragmentation behavior is qualitatively consistent with theoretical predictions and previous reports on nanowires undergoing Rayleigh decay.[77,79,81]
FESEM images in Figure 5.4 demonstrate the morphological changes observed after exposure to elevated temperatures. At T_h=1000 °C (t_h=30 min) nanowires with an average diameter of 30 nm transformed into linear chains of spheres showing regular distances between adjacent spheres (Figure 5.4a). The micrograph in Figure 5.4b depicts a 30 nm diameter Pt nanowire that fragmented in segments of varying length after annealing at 900 °C for 30 min. The two peanut-shaped segments (framed) are about to separate into three or two spheres, respectively, and demonstrate particularly well the fragmentation process and the changes during sphere formation.
Nichols described two different modes of transformation depending on the aspect ratio of the cylindrical rod: Below a certain length-to-diameter ratio only one spherical particle is formed, while for values

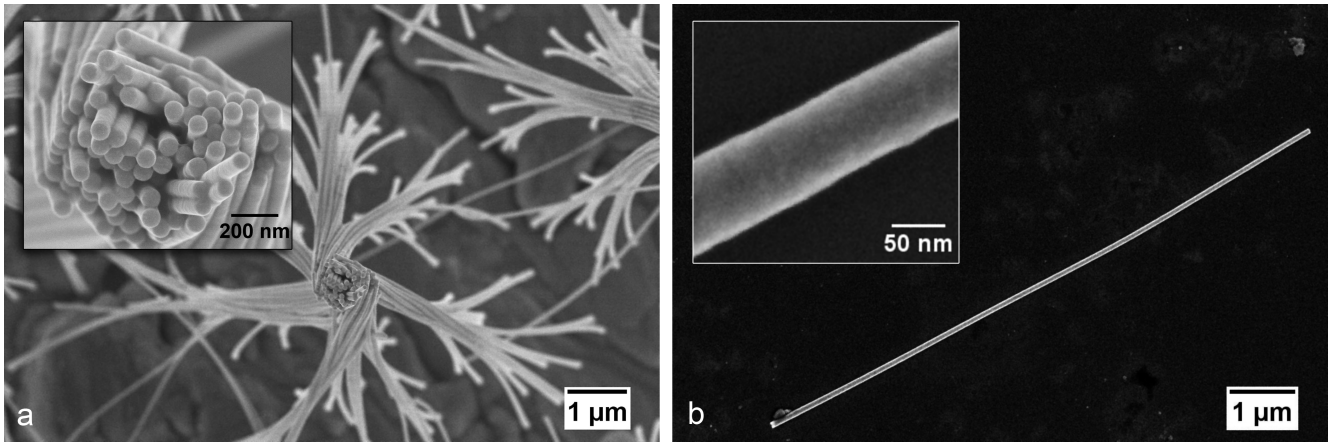

Figure 5.3: SEM images of nanowires (R_0=74 nm) produced for the investigation of the thermal stability. (a) Nanowires still connected to the cathode layer after the polymer matrix has been removed. The front faces of the wires are depicted in the inset. (b) A nanowire on a silicon wafer. The inset shows the cylindrical wire at higher magnification.

higher than the critical ratio two or more spheres are created.[152] These predictions are supported by experimental results.
Besides the breakup into equally sized spheres so-called satellite drops are observed. Satellite particles are much smaller than the main particles and are found only infrequently.[140] In Figure 5.4c a satellite (encircled) particle between main particles in a chain of spheres is depicted. The formation of such small particles is based on a breakup morphology that is different from the normally observed form (Figure 5.4b), which results in particles of same size. Satellite drops originate from two particles separating with an elongated neck between them.

Influence of impurities

Figure 5.5 presents several 74 nm diameter nanowires after annealing at 900 °C for 30 min. Although the nanowires are in close vicinity, the wires feature fragmentation to a varying degree. The insets show two wires at higher magnification and clearly reveal their morphology. The nanowire in the center exhibits definitive indication of perturbations, but did not fragment, whereas the wire in the lower right corner decayed already into shorter segments and even spheres along the total wire length. Responsible for the increased instability against Rayleigh decay are impurities, which can by identified as a dark area around the fragmented wire. These impurities are probably polymer residues, but could also arise from the used solvent, and accumulate in certain areas when the solvent forms increasingly smaller drops while being evaporated. It is not known whether the impurities directly enhance the surface diffusion of the wire atoms or improve the thermal contact between the nanowire and the substrate, and thus increase the temperature and decay rate.

Of course, nanowires affected by impurities must not be considered for systematic evaluations of decay processes. Fortunately, already very small amounts of impurities can be detected by high-resolution imaging.

Changes as a function of temperature

To study the effect of temperature on the morphology of cylindrical nanostructures, nanowires were heated at different temperatures T_h=600, 700, 800, 900, and 1000 °C for 30 min. Figures 5.6b-f show a representative sequence of 30 nm diameter nanowires imaged after the controlled annealing experiment. In Figure 5.6a the cylindrical shape of a nanowire prior to annealing is depicted. The wires show different

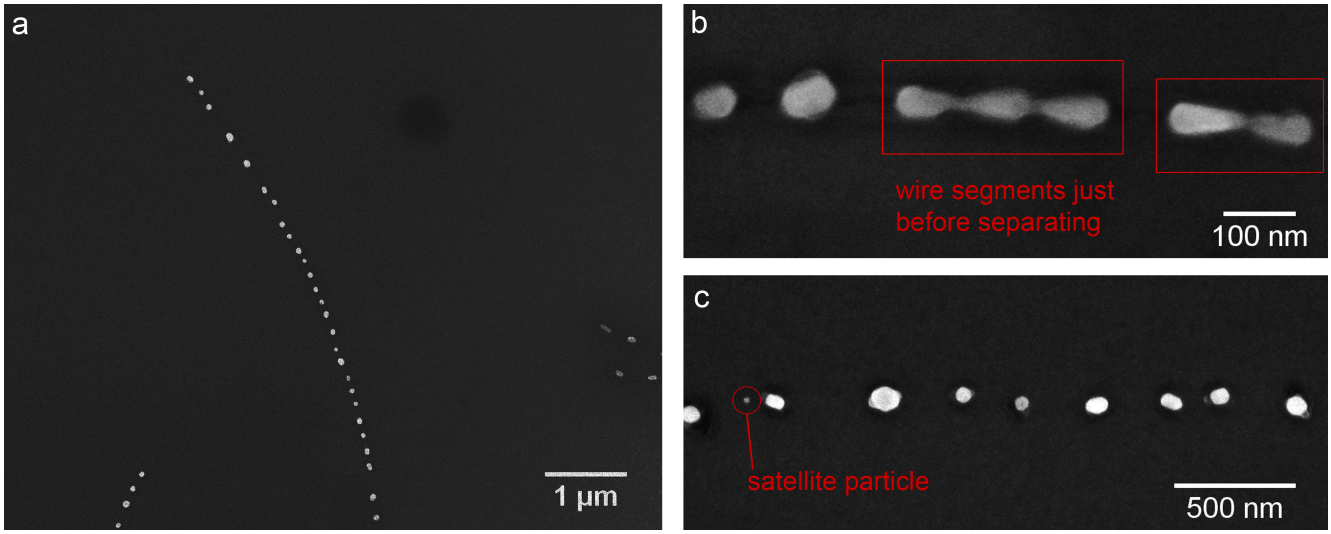

Figure 5.4: FESEM images of nanowires after annealing at elevated temperatures. (a) Low-magnification image of nanowires with an average diameter of d=30 nm that completely transformed into chains of spheres at T_h=1000 °C. (b) At T_h=900 °C nanowires (d=30 nm) transform into shorter segments and spheres. The two framed segments are about to transform into two and three spheres, respectively. (c) Rarely, satellite particles (encircled), which are much smaller than the main particles, are found in sphere chains (T_h=1000 °C, d=30 nm).

stages of Rayleigh decay. With increasing temperature the cylindrical geometry transforms progressively into a thermodynamically favored spherical one.

After annealing at 600 °C, nanowires show radial perturbations along the wire axis resulting in the deviation from the cylindrical shape (Figure 5.6b). Numerous symmetric diameter constrictions can be identified, but also a few unsymmetrical perturbations occur. However, the wires did yet not decay into shorter segments. Wires that had been annealed at 700 °C fragmented into sections with lengths of several hundred nanometers (Figure 5.6c). At this temperature fluctuations of the diameter are additionally more pronounced. The average diameter, especially in the case of relative short segments, apparently increased. After annealing at 800 °C, short segments that are often peanut-shaped and are about to separate into several spheres, as well as shorter segments of up to approximately 200 nm are observed (Figure 5.6d). At this stage, the process of decay seems to be easily predictable. After heating at 900 °C, Pt nanowires fragmented into a chain of particles that consists roughly to equal parts of cylindrical and spherical nanoparticles. In the representative image shown in Figure 5.6e the cylindrical segments are very short allowing only a separation into two spheres at most. Transformation into spherical particles is almost completed. Finally at 1000 °C, the wires decayed, due to Rayleigh instability, to chains of spheres with rather regular sphere-to-sphere distances along the total wire length. The transformation process proceeded homogeneously for all wires on the substrate surface.

Although many symmetrical diameter constrictions are visible in the initial stage of transformation after annealing at 600 °C, fragmentation into segments of varying length that are much longer than the average distance of perturbations are observed for annealing experiments at higher temperatures (T_h=700 °C). These findings might be explained by different growth rates of perturbations.

Changes as a function of diameter

The development of the decay process driven by Rayleigh instability is similar for nanowires with larger diameters except for the fact that the fragmentation process is slower at the same temperature. Sequences of 50 and 74 nm diameter nanowires undergoing Rayleigh decay at different temperatures

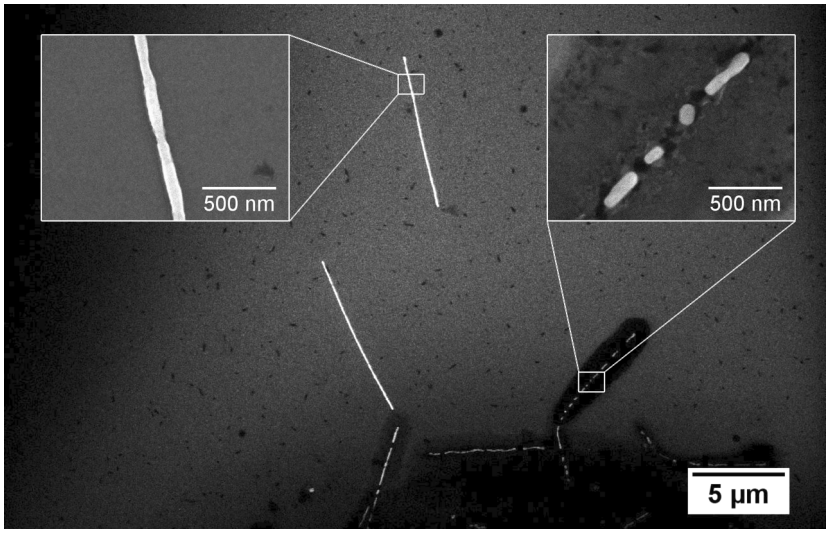

Figure 5.5: Influence of impurities on the fragmentation of nanowires at elevated temperatures (T_h=900 °C, d=74 nm).

T_h show a qualitatively comparable fragmentation behavior as observed for the 30 nm nanowires (Supporting information, Figures S2-S3).
Wires with different diameters that were annealed at the same conditions show a variation in fragmentation morphology. In Figure 5.7 nanowires with d=30, 50, and 74 nm are depicted after being heated to T_h=600 and 900 °C, respectively, for 30 min. At 600 °C the thinnest wires already exhibit obvious indications of transformation processes, while the 50 nm wires show only slight deviations from the cylindrical shape; the thickest nanostructures were practically not deformed (Figures 5.7a-c). Annealing at 900 °C resulted in considerable changes for all regarded nanowires (Figures 5.7d-f). The nanowires fragmented into sections of varying length. The average length of these shorter segments depends on the initial diameter as supported by the representative micrographs. The 30 nm diameter nanowires form a chain of very short fragments and spheres after annealing, whereat the thicker nanowires decayed into increasingly longer segments.
Theoretical predictions by Nichols and Mullins state that the instability of a cylinder strongly depends on its diameter and is proportional to R_0^4. In this respect, the experimental results are consistent with the theory, because nanowires with larger diameters, that were annealed at the same conditions, do not show morphological changes to the same degree.

The Rayleigh decay for Pt nanowires is similar to simulations and experimental works reported for metal nanowires in terms of morphological changes, except for the fact that various metal nanowires of comparable diameter require different temperatures to decay.[76,77,79]
For example, 25 nm diameter Au nanowires developed diameter fluctuations by annealing at 300 °C for 30 min.[79] At 500 °C they completely transformed into a chain of spheres. Toimil-Molares et al. investigated Cu nanowires with diameters of 30-50 nm.[77] They found that Cu nanowires start to fragment during annealing at 400 °C for 30 min and form chains of nanospheres at 600 °C. The decay temperature T_d of the different metal nanowires seems to be correlated to the melting point T_m of the corresponding bulk material. In the case of Cu nanowires, the decay process might be influenced in addition by the formation of a thin oxide layer. However, comparing the polycrystalline noble metal Au and Pt nanowires, which show same bond type and face centered cubic (fcc) crystal structure, morphological changes start to form for both at ≈0.43 T_m.[153] Surprisingly, the same value is obtained for both metal nanowires although the decay temperature T_d was determined rather inaccurately (Table 5.2). T_d is here defined as the temperature at which first signs of decay are visible. It has to be considered that T_d is slightly underestimated for the Au nanowires in comparison to the Pt structures because the Au wires are 2.5 nm

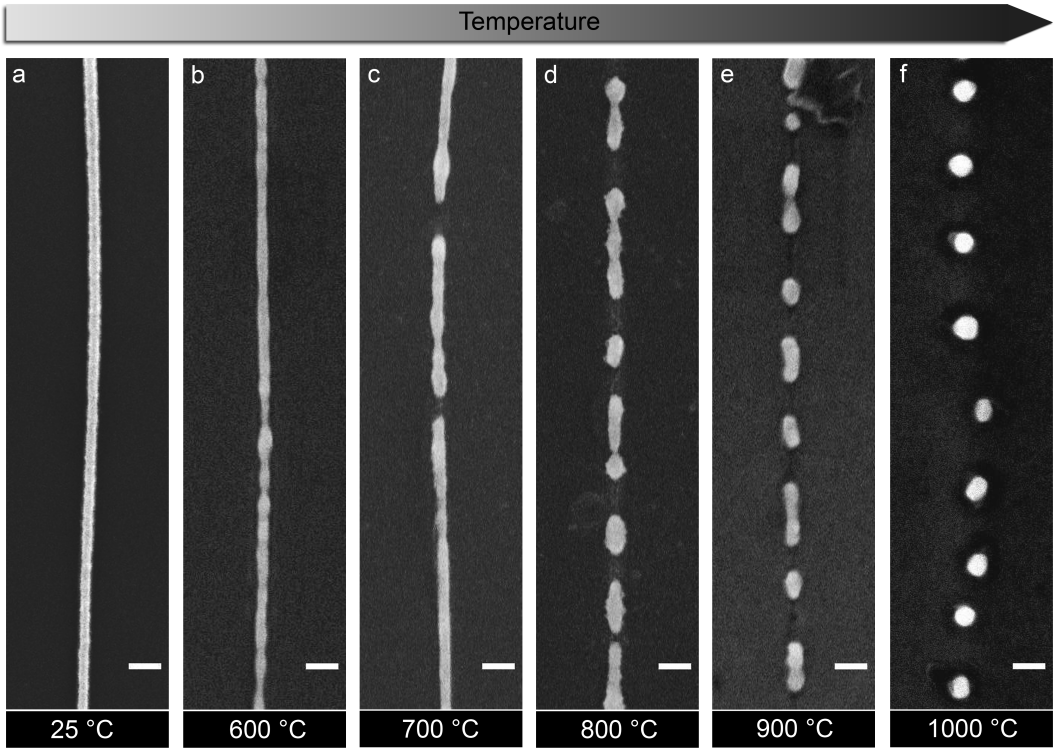

Figure 5.6: SEM images of nanowires (d=30 nm) undergoing fragmentation as function of temperature. Nanowires were heated at different temperatures T_h=600, 700, 800, 900, and 1000 °C for t_h=30 min. The as-prepared cylindrical nanowires (a) are more and more transformed (b-e) as the temperature is increased and finally decay into a chain of spheres (f). All scale bars are 100 nm.

Table 5.2: Correlation of decay temperature T_d with melting point T_m for 25-30 nm diameter Au and Pt nanowires.[79]

Metal	Structure	T_m [K]	T_d [K]	T_d/T_m
Au	polycrystalline (fcc)	1336	573	0.429
Pt	polycrystalline (fcc)	2046	873	0.427

smaller in radius. Of course there is not enough data available, but it might be possible that a general rule can be developed with additional experiments.

Comparison with theoretical predictions

Pt nanosphere chains, obtained by annealing of Pt nanowires of different diameters at 1000 °C for 30 min, were investigated by FESEM to determine the average distances between adjacent spheres λ_s and the average diameters of the spheres d_s. At least 15 chains were measured for each diameter. The results are depicted as a function of the initial diameter R_0 in Figure 5.8 together with the theoretically predicted values, which are λ_{max} and $d_{s,theo}$ ($= \sqrt[3]{6\lambda_{max}R_0^2}$) for the average sphere spacing and the average sphere diameter, respectively. The exact values are also given in Table 5.3. For calculations, surface diffusion was assumed to be the determining transport process.

In Figure 5.8a the experimentally obtained values for the sphere spacing (blue circles) are always much larger than the spacings that were calculated using the model by Mullins and Nichols (red squares). The experimental data are not only 1.8-2.3 times larger than the predicted values but also exhibit a distinct

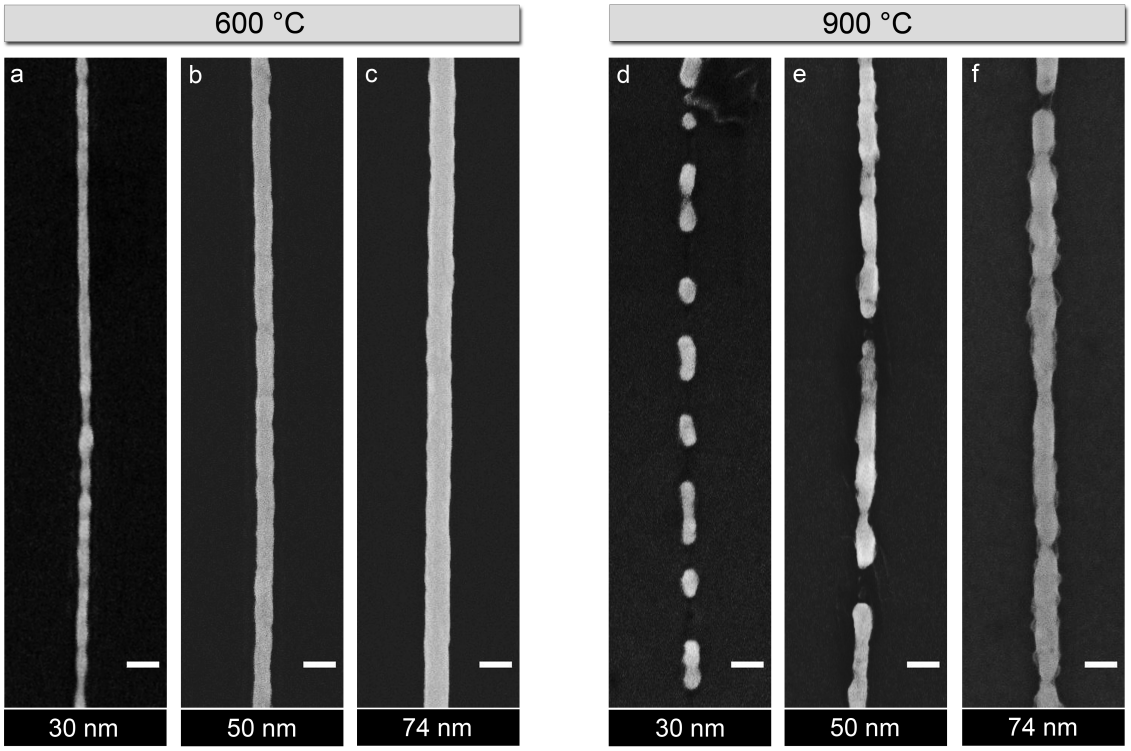

Figure 5.7: SEM images of nanowires (R_0=30, 50, 74 nm) undergoing fragmentation at different temperatures T_h=600 (a-c) and 900 °C (d-f). The scale bars are 100 nm. Nanowires with different diameters show different fragmentation morphologies after annealing at same conditions because instabilities strongly depend on size.

scatter showing a standard deviation of 29-39%. The distribution of λ_s is much larger than the diameter distribution of the wires, which is 9-10%. The same behavior is observed for the diameter of the spheres because d_s is correlated to λ_s due to volume conservation (Figure 5.8b). The average diameters are 21-25% larger than $d_{s,theo}$ and have comparable standard deviations.

As origin of the deviation of λ_s from the predicted value of λ_{max} may be responsible an anisotropic surface energy of the Pt wires, which is a direct consequence of the polycrystalline wire structure. Nichols and Mullins assumed isotropic surface energy and surface diffusion as main transport process resulting in $\lambda_{max} = 8.89R_0$. It is not surprising that the Pt nanowires, consisting of small crystallites with random orientation, show a deviation from the predicted value. The crystallites expose various crystal faces at the wire surface which have different surface energies. Consequently, diffusion proceeds at different rates on individual crystallite surfaces. In addition, the high number of grain boundaries hinders diffusion processes along the cylinder surface. Other transport mechanisms than pure surface diffusion must be considered (e. g., grain boundary diffusion) in this case. Moreover, it has to be considered that the substrate can increase the stability of nanowires against morphological changes as reported previously.[79] The increased average spacings between the Pt nanospheres of $\lambda_s = 16.1\ R_0$ clearly demonstrate a higher stability of the Pt nanowires in comparison to the Nichols and Mullins model. The tranformation process slower than theoretically predicted. Also for polycrystalline Au nanowires higher values for both λ_s and d_s have been reported.[79]

Morphological changes driven by Rayleigh instability can also by regarded as a method for controlled nanostructuring. With cylindrical nanowires of uniform and constant thickness and the appropriate experimental conditions, the fabrication of well-defined chains of nanospheres is possible as demonstrated elsewhere.[76,77]

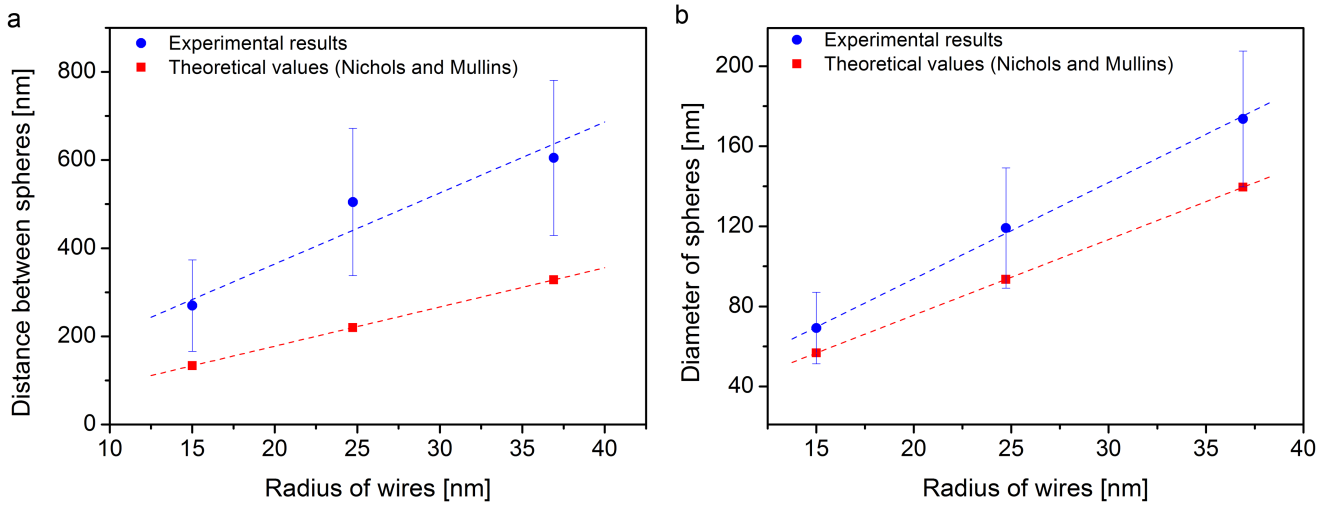

Figure 5.8: Experimentally obtained values in comparison to the model of Nichols and Mullins for nanowires with different initial radii after fragmenting into spheres. (a) Average spacing between adjacent spheres λ_s versus the initial radius of the wires. (b) Average diameter of spheres d_s versus the initial radius of the wires.

Table 5.3: Average diameter d_s and spacing λ_s of spheres obtained by Rayleigh decay of Pt nanowires of different diameters. The wires were annealed at 1000 °C for 30 min. In adddition to the experimental results, calculated values for the theoretically predicted spacings (λ_{max}) and diameters of spheres ($d_{s,theo}$) are given.

R_0 [nm]	λ_s [nm]	λ_{max} [nm]	d_s [nm]	$d_{s,theo}$ [nm]
15.0	270 ± 104	133	69 ± 18	57
24.7	505 ± 167	220	119 ± 30	93
36.9	605 ± 176	328	174 ± 33	139